16th World Conference on Earthquake, 16WCEE 2017

Santiago Chile, January 9th to 13th 2017

Paper N° 4130

Registration Code: S-Q1461030666

HYSTERETIC PERFORMANCE STUDY ON A PRE-PRESSED SPRING SELF-CENTERING ENERGY DISSIPATION BRACE

Long-He.Xu[(1)], Xiao-Wei.Fan[(2)], Zhong-Xian.Li[(3)]

(1) Professor, School of Civil Engineering, Beijing Jiaotong University, Beijing 100044, China. lhxu@bjtu.edu.cn
(2)Ph.D Candidate, School of Civil Engineering, Beijing Jiaotong University, Beijing 100044, China. 15115317@bjtu.edu.cn
(3) Professor, Key Laboratory of Coast Civil Structure Safety of China Ministry of Education, Tianjin University, Tianjin 300072, China. zxli@ tju.edu.cn

Abstract

This paper presents a new type of pre-pressed spring self-centering energy dissipation (PS-SCED) bracing system that combines friction energy dissipation mechanisms between the inner and outer tube members with the pre-pressed combination disc springs that are installed on both ends of the brace to provide the self-centering capability. The mechanics and the equations governing the design and hysteretic responses of the bracing system are outlined, and a series of validation tests of a large scale PS-SCED bracing specimen were conducted due to the low cyclic reversed loadings. Experimental results demonstrate that the proposed bracing system exhibits a stable and repeatable flag-shaped hysteretic response with excellent self-centering capability, appreciable energy dissipation, large ultimate bearing and deformation capacities. Almost no residual deformation occurs when the friction force is less than the initial pre-pressed force of disc springs. Results also show that the compressive capability is better than the tensile capability and the ductility behavior in tension is better than that of the brace in compression, and the proposed bracing system still can reduce the influence of residual deformations and dissipate energy effectively even the tubes are already in the elastic-plastic stage. The overall hysteretic responses are well predicted by the proposed equations and good agreements between the calculated and experimental bearing forces are found.

Keywords: self-centering energy dissipation brace; combination disc spring; hysteretic behavior; residual deformation; low cyclic reversed loading test

1. Introduction

Conventional earthquake-resistant structural systems, such as moment-resisting frames, shear wall structures or concentrically braced systems, are expected to provide adequate safety and experience large inelastic deformations for design level earthquakes, which will inevitably cause the structural damage and the occurrence of residual deformations. Because of the structural damage and residual deformations, some buildings are difficult to repair and have to be demolished and rebuilt, which results in huge economic losses and also affects the normal use. It is advantageous to develop the system with capability of energy dissipation to reduce the structural damage, and with capability of self-centering to return to its initial position after an earthquake, such as those systems exhibiting flag-shaped hysteretic responses. The moment-resisting frames with steel post-tensioned self-centering connections and supplemental energy dissipation devices were developed and verified by several researchers through simulation and experiments[1-5], and these connections were able to undergo large deformations with good energy dissipation and self-centering capabilities.

Conventional braces which are designed according to the latest earthquake-resistant design standards are deemed to provide adequate seismic safety for structures during earthquakes, buckling restrained braces (BRBs), which are able to yield in both tension and compression, have been developed to overcome the buckling of conventional braces [6-7], however, large residual deformations occur in BRBs and structures after moderate earthquake[8-9]. To address these drawbacks, some self-centering braces with flag-shaped hysteretic performance were developed [10-12], which utilized the superelastic shape memory alloy rods or pre-stressed steel strands to provide the self-centering capability to reduce or eliminate the residual deformations. Christopoulos et al. [13] proposed a self-centering energy dissipation brace which used friction devices to dissipate energy, and a set of fiber-reinforced polymer tensioning elements to provide self-centering capacity. A reusable hysteretic damping brace with the energy dissipation component made up of superelastic Nitinol wires or friction devices was developed by Zhu et al. [14], which exhibited self-centering hysteretic responses and outstanding fatigue properties. Seismic analyses of braced frames have confirmed that the structures with self-centering energy dissipation braces have smaller residual deformations than those systems with BRBs after earthquakes [15-16].

In this paper, a new type of pre-pressed spring self-centering energy dissipation (PS-SCED) bracing system that combines friction energy dissipation mechanisms with the pre-pressed combination disc springs is developed. The configuration and mechanical behaviors of PS-SCED bracing system are described, and experiments of a large scale brace specimen are conducted due to the low cyclic reversed loadings to demonstrate the behaviors of bracing system.

2. Mechanics of PS-SCED brace

The PS-SCED bracing system consists of two tube members, the outer tube and inner tube, which can slide past each other, the pre-pressed disc springs that provide the self-centering force, and friction energy dissipation mechanisms (FEDMs), as shown in Fig.1. Four pieces of steel plates are welded to the inner tube to improve the bearing and deformation capabilities of bracing system, and several blocking plates are welded to the two tube members to extrude the combination disc springs to increase the self-centering capability. The FEDMs are connected to the two tube members and activated when the relative motion occurs between the two members. The initial pre-pressed force of combination disc springs and friction force of FEDMs provide the bearing force of the bracing system for normal service condition. Once the relative motion between the two tubes occurs, the friction force of the FEDMs changes from static friction to kinetic friction force to dissipate the input energy, the compression deformation of disc springs increases regardless the brace is in compression or in tension. If the initial pre-pressed force of disc springs can overcome the force desired to activate the FEDMs, a full self-centering behavior can be achieved.

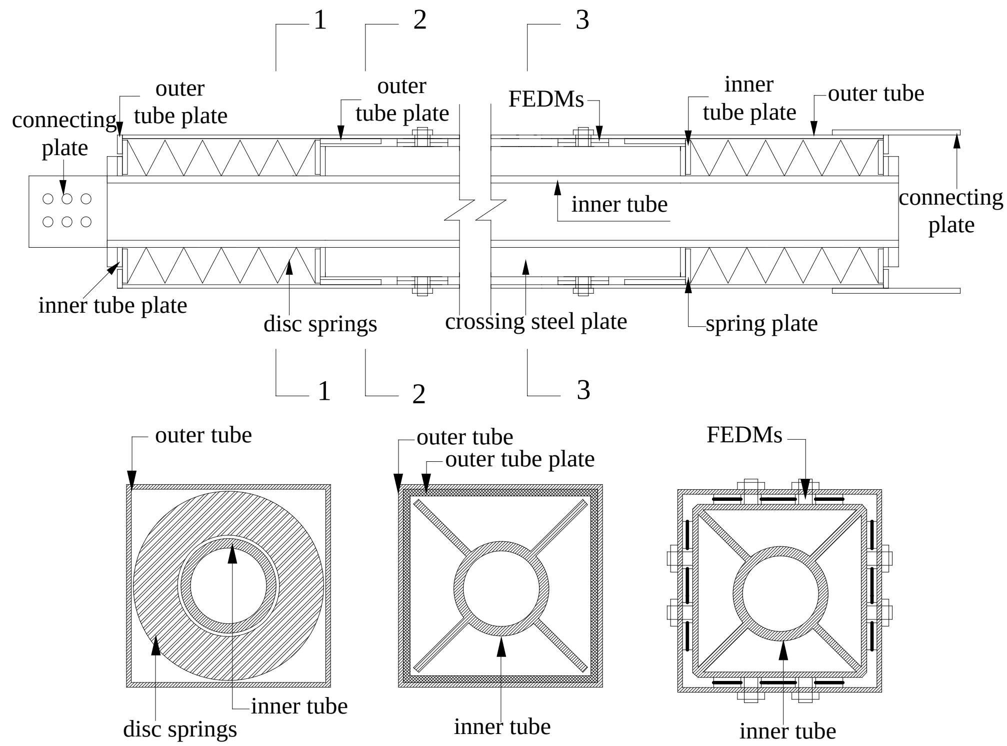

Fig. 1 Configuration of PS-SCED brace

The PS-SCED bracing system is expected to exhibit a repeatable flag-shaped hysteretic response with full self-centering capability, Fig.2 shows the hysteretic response of brace under one circle of horizontal low cyclic reversed loading. The hysteretic responses are divided into different stages in tension or compression according to the changes of stiffness. The system in tension experiences four stages, OA stage as shown in Fig.2, the relative motion between the two tubes doesn't occur, the stiffness of inner or outer tube is considerably larger than that of one side of disc springs, and the deformation of brace is mainly determined by two tube members, thus the stiffness of the whole brace, K_1, is given by,

$$K_1 = \frac{K_i \cdot K_o}{K_i + K_o} \tag{1}$$

where K_i and K_o are the axial stiffness of the inner and outer tube, respectively.

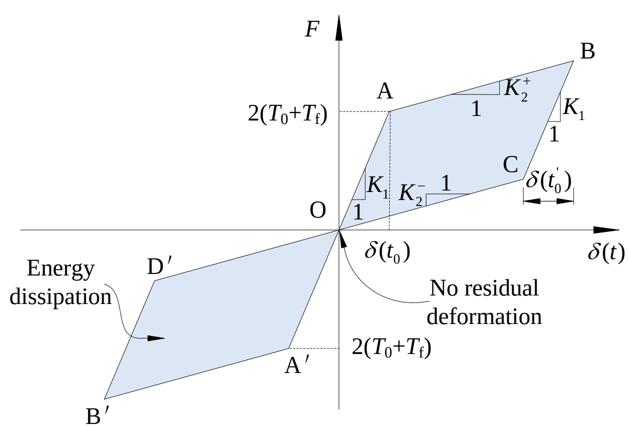

Fig. 2 Flag-shaped hysteretic behavior of PS-SCED brace

AB stage, the relative motion between the two tube members starts to the target deformation, the stiffness of the brace, K_2^+, is mainly controlled by the combination disc springs, which is approximately equal to the stiffness of springs,

$$K_2^+ = 2U_f^+ K_s \tag{2}$$

$$U_f^+ = \frac{1}{1 - U_M(n-1) - U_R} \tag{3}$$

where K_s is the stiffness of one side of combination disc springs, U_f^+ is the friction coefficient of disc springs when the PS-SCED brace is loaded, n is the number of the same specification disc springs at the same direction, U_M is the friction coefficient of disc spring cone, and U_R is the friction coefficient at the bearing edge of disc springs.

BC stage, the bracing system begins to unload, and the relative motion between the two tube members doesn't occur because of the friction of combination disc springs and FEDMs, which is similar to the first stage, OA stage, the stiffness of the brace, K_1, is mainly controlled by two tube members.

CO stage, the bracing system is in the self-centering stage which is similar to the second stage of loading, AB stage, and the stiffness of the whole brace, K_2^-, is given by,

$$K_2^- = 2U_f^- K_s \tag{4}$$

$$U_f^- = \frac{1}{1 + U_M(n-1) + U_R} \tag{5}$$

where U_f^- is the friction coefficient of disc springs when the PS-SCED brace is unloaded.

The PS-SCED bracing system in compression also experiences four stages, OA', A'B', B'C', C'O stage, as shown in Fig.2, the mechanical behaviors are similar to that of the bracing system in tension. For the proposed bracing system to function, two tube members must be capable of bearing significant axial forces without failure or yielding and the combination disc springs should have enough stiffness to produce the restoring force that is required to assure the self-centering capacity of the system.

According to the elastic deformation of the inner and outer tubes, the bilinear elastic model of combination disc springs and the ideal elastic-plastic model of friction devices, the restoring force of PS-SCED brace in tension can be obtained as follows,

$$F = \begin{cases} K_1\delta(t) & 0<\delta(t)<\delta(t_0) \text{ and } \delta(t)\cdot\dot{\delta}(t)>0 \\ K_1\delta(t_0) + K_2^+\left(\delta(t)-\delta(t_0)\right) & \delta(t_0)<\delta(t)<\delta(t_{\max}) \text{ and } \delta(t)\cdot\dot{\delta}(t)>0 \\ K_1\left(\delta(t_0)+\delta(t)-\delta(t_{\max})\right)+ & \delta(t_{\max})-\delta(t_0^{'})<\delta(t)<\delta(t_{\max}) \\ \quad K_2^+\left(\delta(t_{\max})-\delta(t_0)\right) & \text{and } \delta(t)\cdot\dot{\delta}(t)<0 \\ K_1\left(\delta(t_0)-\delta(t_0^{'})\right)+K_2^+\left(\delta(t_{\max})-\delta(t_0)\right)- & 0<\delta(t)<\delta(t_{\max})-\delta(t_0^{'}) \\ \quad K_2^-\left(\delta(t_{\max})-\delta(t_0^{'})-\delta(t)\right) & \text{and } \delta(t)\cdot\dot{\delta}(t)<0 \end{cases} \tag{6}$$

where

$$\delta(t_0) = \frac{2(T_0+T_f)}{K_1} \tag{7}$$

$$\delta(t_0^{'}) = \frac{T_0\left(U_f^{+} - U_f^{-}\right) + K_2^{+}\left(\delta(t_{\max}) - \delta(t_0)\right) - K_2^{-}\left(\delta(t_{\max}) - \delta(t_0)\right) + 4T_f}{K_1}$$

(8)

where T_0 is the initial pre-pressed force of one side of disc springs, T_f is the friction force provided by one side of friction devices, $\delta(t)$ is the deformation of the PS-SCED brace in compression or in tension, $\delta(t_0)$ is the maximum deformation of brace before the relative motion between the two tube members occurs when the bracing system is loaded, and $\delta(t'_0)$ is the maximum relative deformation of brace before the relative motion between the two tube members occurs when the bracing system is unloaded, $\delta(t_{\max})$ is the maximum target deformation of brace.

When the residual deformation, δ_r, occurs, it is given by,

$$\delta_r = \frac{K_1\left(\delta(t_0^{'}) - \delta(t_0)\right) - K_2^{+}\left(\delta(t_{\max}) - \delta(t_0)\right)}{K_2^{-}} + \delta(t_{\max}) - \delta(t_0^{'}) \qquad (9)$$

3. Hysteretic behavior tests of PS-SCED bracing system

A large-scale PS-SCED brace specimen was fabricated and tested on a 3,000kN servo hydraulic test system in the Structural Laboratory at Beijing University of Technology. As shown in Fig.3, the specimen consists of a 215×215×6mm box shaped outer tube and a circular inner tube with 108mm outer diameter and 88mm inner diameter, four steel plates with 10mm thickness are welded to the inner tube to improve the bearing capacity and stability of the bracing system and several blocking plates are welded to the inner and outer tubes to enhance bearing force and push or pull the combination disc springs, besides the outer tube is Q235 steel, the inner tube and blocking plates are Q345 steel, and the overall length of this specimen is 1680mm. Total 32 pieces of disc springs with 200mm outer diameter, 112mm inner diameter, 16.2mm height and 12mm thickness and 4.2mm solid height are used to produce the expected restoring force for the bracing system and the pre-pressed force is 270kN. Eight friction devices, which are equipped with non-asbestos organic (NAO) friction pads with the dimension of 134×80×6mm, are used to dissipate the input energy, and the initial friction forces are adjusted to 150kN, 200kN, and 300kN, respectively, by changing the pre-tension force of high-strength bolts. The bearing forces of PS-SCED brace are measured by the load cell installed in the test machine, and the deformations of brace are measured using two displacement meters that are installed on the brace.

Fig. 3 Test setup of PS-SCED brace specimen

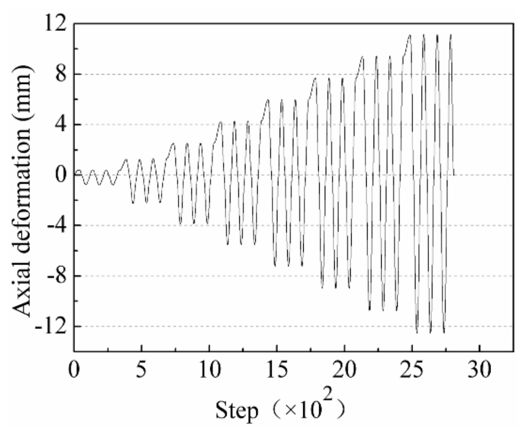

Fig. 4 Loading scheme of PS-SCED brace

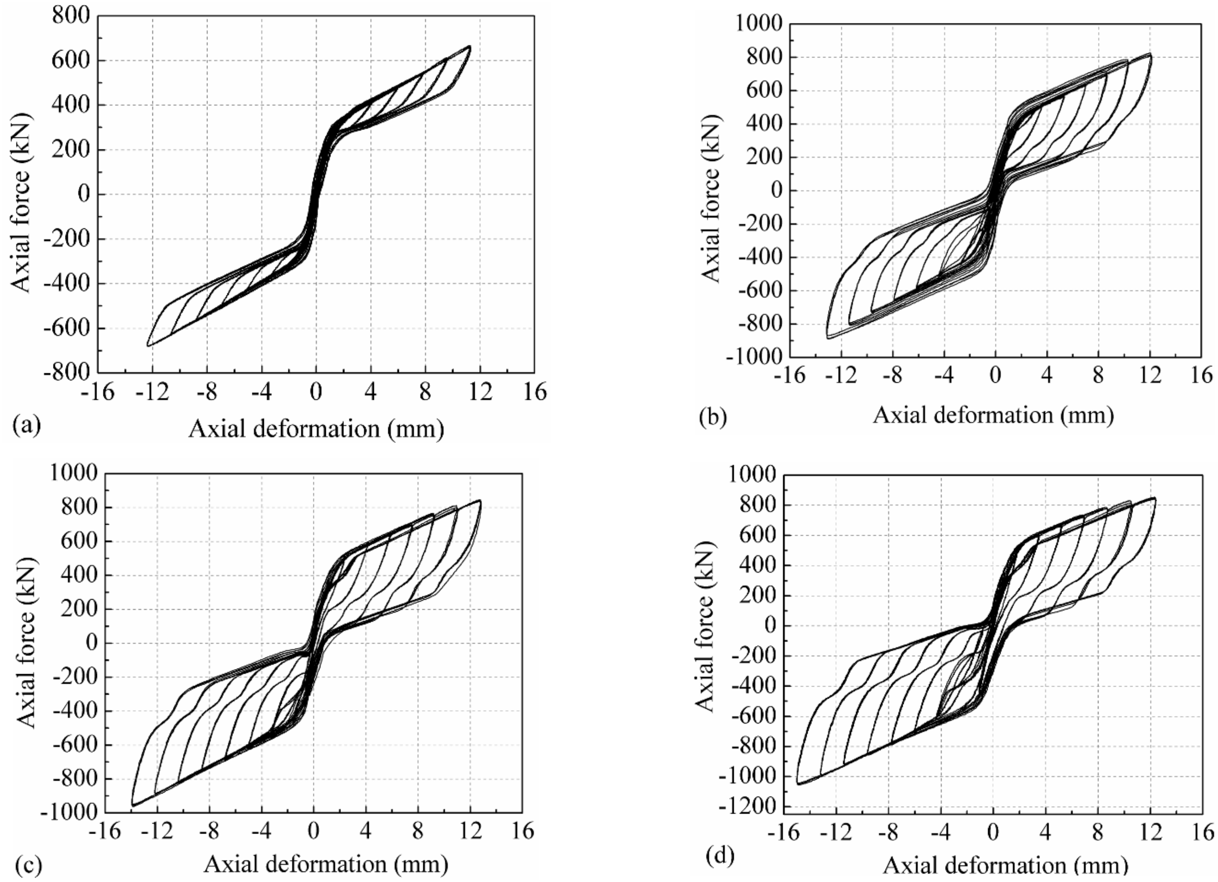

Fig. 5 Hysteretic responses of PS-SCED brace with friction force of (a) 0kN, (b) 150kN, (c) 200kN, and (d) 300kN

Fig.4 shows the low cyclic reversed loading scheme, and the hysteretic responses of specimen with different friction forces are shown in Fig.5. It is observed that the PS-SCED brace exhibits flag-shaped hysteretic responses with excellent self-centering capability, the energy dissipation is enhanced by increasing the friction forces of FEDMs, and almost no residual deformation occurs when the friction force is less than the pre-pressed force of combination disc springs, as shown in Figs.5 (b)-(c). However, the residual deformation of the brace specimen appears when the friction force is larger than the pre-pressed force of combination disc springs, as shown in Fig.5 (d), which is about 1.5mm and only accounts for 12% of the maximum displacement of the brace. Therefore, the PS-SCED bracing system displays a stable and repeatable self-centering response with effective energy dissipation throughout the loading protocol.

Fig.6 shows the skeleton curves of the specimen with different friction forces, when the relative motion occurs between the two tube members, the stiffness of PS-SCED bracing system changes from the first stiffness that is controlled by the inner and outer tube members to the second stiffness, which is controlled by combination disc springs, and the whole PS-SCED brace is in elastic state throughout the loading protocol.

To study the ultimate bearing capacity and ductility properties of the proposed PS-SCED brace, the experiments of specimen with pre-pressed force of 270kN and friction force of 240kN were conducted, Fig.7 shows the buckling of connecting plates of the brace specimen in compression, and the hysteretic responses and the skeleton curve are shown in Figs.8-9, respectively. The specimen in tension exhibits a full flag-shaped hysteretic response with effective energy dissipation and eliminates the residual deformation before the loading displacement reaches 12mm, and the residual deformation occurs and increases with the increase of deformation of brace when the loading displacement increases from 12mm to 28mm, which is 9.2mm and accounts for 32.9% of the maximum target tensile deformation. The PS-SCED brace in compression also exhibits a full flag-shaped hysteretic response before the loading displacement reaches 24mm which is the solid height of combination disc springs, with the increase of loading displacement, the controlled stiffness of brace changes from combination disc springs to the two tube members, thus the second stiffness increases suddenly, and the residual deformation occurs and starts to increase, which is about 23.2% of the maximum target compressive deformation. In addition, the PS-SCED bracing system still can reduce the influence of residual deformations and dissipate energy effectively even the inner and outer tubes are already in the elastic-plastic stage.

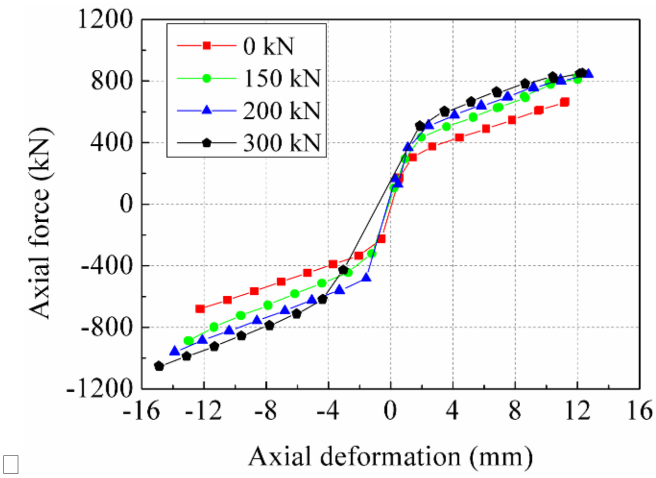

Fig. 6 Skeleton curves of PS-SCED brace with different friction forces

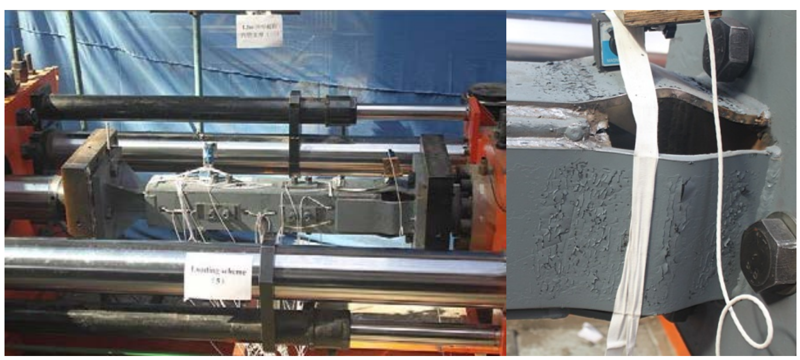

Fig. 7 Buckling of connecting plates of PS-SCED brace

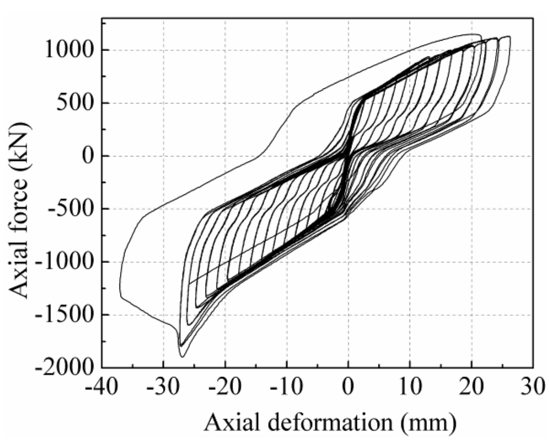

Fig. 8 Hysteretic responses of PS-SCED brace

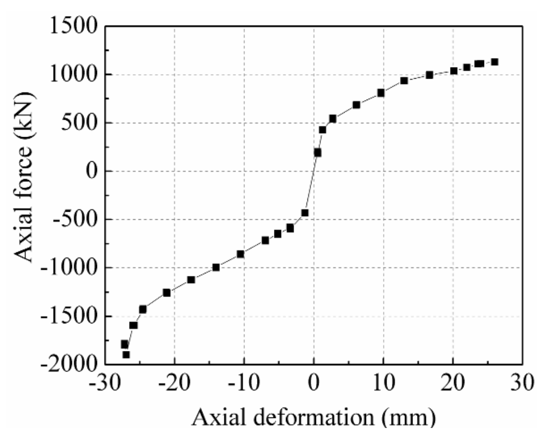

Fig. 9 Skeleton curve of PS-SCED brace

The ultimate bearing forces of PS-SCED brace specimen are -1770kN in compression and 1080kN in tension, which have exceeded the design capacity of 954kN, respectively, and the compressive capability is better than the tensile capability because the loads can be distributed to each part of the inner and outer tube members by the bracing system, and the ductility behavior in tension is better than that of the brace in compression. As a result, the ultimate compressive bearing capacity of the PS-SCED bracing system is determined by the bearing capacity of the two tube members and the compressive force of combination disc springs to reach the target deformation, and the strength and stability of the connecting plates should be satisfied the requirements of the ultimate bearing capacity.

4. Comparison of prediction and test results

To verify the accuracy of the predictive equations governing the response of the PS-SCED bracing system, comparative analysis of prediction and test results for hysteretic responses of the specimen with the initial pre-pressed force of 270kN and friction force of 0kN, 150kN, 200kN, and 300kN are carried out, and the error is defined as Eq. (10) to further quantify the accuracy of the prediction.

$$J_{\mathrm{error}} = \frac{\max\left|F_{\mathrm{pre}} - F_{\mathrm{test}}\right|}{\max\left|F_{\mathrm{test}}\right|}\% \tag{10}$$

where F_{pre} and F_{test} are the bearing force of the bracing system corresponding to the loading scheme during the prediction and experiments, respectively.

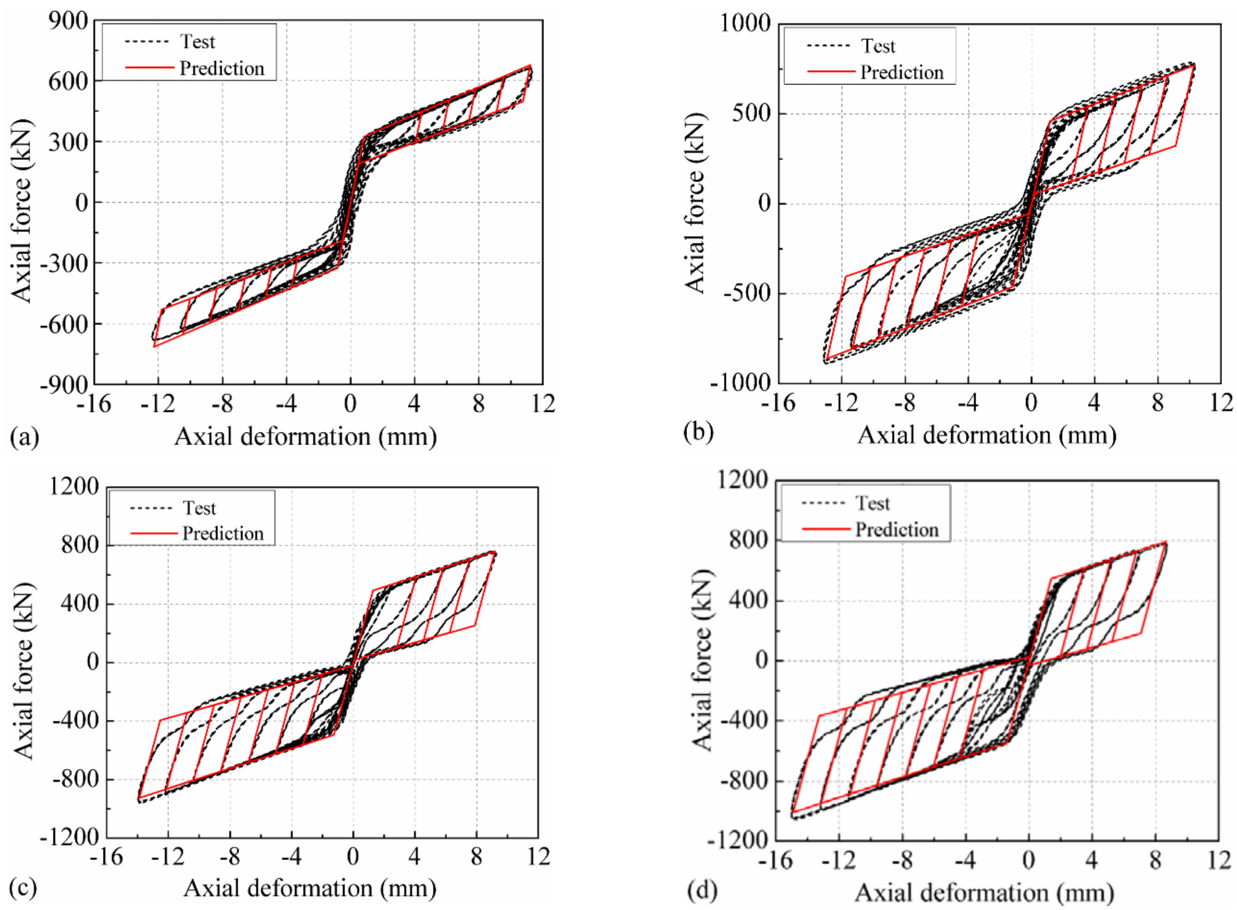

Fig. 10 Comparison of the predicted and tested hysteretic responses of PS-SCED brace with friction force of (a) 0kN, (b) 150kN, (c) 200kN, and (d) 300kN

Fig.10 shows the comparison between the predicted and tested hysteretic responses of the PS-SCED brace specimen, and the maximum bearing forces of the system corresponding to the loading displacement and the errors between the prediction and tests are listed in Table 1. It is indicated that the predictive equations can accurately portray the mechanical behaviors of the PS-SCED bracing system, and the maximum error between the prediction and experiments is about 8.45%, 6.65%, 5.02%, 4.47% corresponding to the friction of 0kN, 150kN, 200kN, and 300kN, respectively. And it confirms that the proposed bracing system performs as predicted by the equations governing its mechanical behaviors.

Table 1 Maximum bearing force and errors of PS-SCED brace between prediction and experiments

Friction force= 0kN												
Disp. (mm)	-12.3	-10.5	-8.8	-7.1	-5.3	-3.7	2.5	4.4	6.2	7.8	9.6	11.2
maxF_{test} (kN)	-679.9	-623.4	-565.1	-504.4	-445.8	-389.2	319.1	433.1	487.8	543.8	612.9	667.4
maxF_{pre} (kN)	-714.5	-653.0	-595.8	-535.1	-477.9	-422.1	331.1	447.3	505.4	561.8	621.7	678.2
J_{error} (%)	5.09	4.75	5.44	6.07	7.19	8.45	3.8	3.31	3.61	3.30	1.42	1.61
Friction force= 150kN												
Disp. (mm)	-12.9	-11.4	-9.7	-7.9	-6.2	-4.5	3.6	5.3	7.0	8.6	10.3	12.1
maxF_{test} (kN)	-888.6	-794.7	-722.8	-659.6	-582.5	-513.7	503.1	568.0	629.4	701.2	776.8	809.2
maxF_{pre} (kN)	-837.1	-783.3	-725.9	-664.5	-606.1	-547.8	518.6	576.9	634.1	688.6	746.4	805.6
J_{error} (%)	5.80	1.43	0.42	0.75	4.05	6.65	3.09	1.56	0.75	1.80	3.92	0.45
Friction force= 200kN												
Disp. (mm)	-13.89	-12.1	-10.4	-8.6	-6.8	-5.1	4.1	5.8	7.5	9.2	11.0	12.7
maxF_{test} (kN)	-955.1	-883.8	-825.2	-755.1	-691.7	-626.2	576.7	644.8	696.8	752.7	798.2	845.2
maxF_{pre} (kN)	-907.2	-847.5	-787.5	-727.4	-666.2	-606.5	573.1	632.4	691.1	747.2	807.8	867.2
J_{error} (%)	5.02	4.12	4.63	3.66	3.69	3.15	0.62	1.91	0.82	0.73	1.21	2.60
Friction force= 300kN												
Disp. (mm)	-14.9	-13.2	-11.3	-9.6	-7.8	-6.1	-4.4	3.5	5.2	6.8	8.6	—
maxF_{test} (kN)	-1048.6	-987.3	-921.4	-853.4	-786.4	-715.1	-620.9	595.7	669.1	733.5	778.3	—
maxF_{pre} (kN)	-1006.9	-946.3	-884.4	-826.2	-764.54	-704.8	-648.6	617.5	675.2	730.1	793.2	—
J_{error} (%)	3.98	4.16	4.02	3.19	2.78	1.45	4.47	3.66	0.91	0.48	1.91	—

5. Conclusions

A new type of PS-SCED bracing system that combines friction energy dissipation mechanisms with the pre-pressed disc springs self-centering mechanism is developed and experimental studied in this contribution. The mechanics and the equations governing the design and hysteretic responses of the bracing system are presented. A series of validation tests of a large scale PS-SCED brace specimen are carried out due to the low cyclic reversed loadings. Experiments of the specimen demonstrate that the bracing system performs as predicted by the equations governing its mechanical behaviors, which exhibits a stable and repeatable flag-shaped hysteretic response with excellent self-centering capability and effective energy dissipation throughout the loading protocol, and good agreements between the calculated and experimental bearing forces are found. Almost no residual deformation occurs when the friction force is less than the pre-pressed force of disc springs. However, the residual deformation of the brace occurs when the friction force is larger than the pre-pressed force of disc springs, which is approximately 12% of the maximum the brace deformation, and it could be controlled by adjusting the ratio of initial pre-pressed force to the friction force. The ultimate bearing capacity experiments indicates that the compressive capability is better than the tensile capability and the ductility behavior in tension is better than that of the brace in compression, and the ultimate compressive bearing capacity of the PS-SCED bracing system is determined by the bearing capacity of the two tube members and the compressive force of disc springs to reach the target deformation. For real application, the strength and stability of the connecting plates should be designed to satisfy the requirements of the ultimate bearing capacity.

Acknowledgements

The writers gratefully acknowledge the partial support of this research by the National Natural Science Foundation of China under Grant No. 51322806 and No. 51578058, the Fundamental Research Funds for the Central Universities under Grant No. 2014JBZ011, and the National Basic Research Program of China (973 Program) under Grant No. 2011CB013606 and 2011CB013603. The content of this paper is part of the paper published on Steel and Composite Structures, an International Journal.

References

[1] Garlock M, Ricles J and Sause R (2005): Experimental studies of full-scale posttensioned steel connections. *Journal of Structural Engineering*, 131(3): 438-448.

[2] Garlock M, Sause R and Ricles J (2007): Behavior and design of posttensioned steel frame systems. *Journal of Structural Engineering*, 133(3): 389-399.

[3] Morgen BG and Kurama YC (2007): Seismic design of friction-damped precast concrete frame structures. *Journal of Structural Engineering*, 133(11): 1501-1511.

[4] Morgen BG and Kurama YC (2008): Seismic response evaluation of posttensioned precast concrete frames with friction dampers. *Journal of Structural Engineering*,134(1): 132-145.

[5] Kim HJ and Christopoulos C (2009): Seismic design procedure and seismic response of post-tensioned self-centering steel frames. *Earthquake Engineering & Structural Dynamics*, 38(3): 355-376.

[6] Sabelli R, Mahin SA and Chang C (2003): Seismic demands on steel-braced frame buildings with buckling-restrained braces. *Engineering Structures*, 25(5): 655-666.

[7] Uang CM, Nakashima M and Tsai KC (2004): Research and application of buckling-restrained braced frames. *International Journal of Steel Structures*, 4(4): 301-313.

[8] Marino EM and Nakashima M (2006): Seismic performance and new design procedure for chevron-braced frames. *Earthquake Engineering & Structural Dynamics*,35(4): 433-452.

[9] Zhu SY and Zhang YF (2007): Seismic behavior of self-centering braced frame buildings with reusable hysteretic damping brace. *Earthquake Engineering & Structural Dynamics*, 36(10): 1329-1346.

[10] Miller DJ (2011): Development and experimental validation of self-centering buckling-restrained braces with shape memory alloy. *Ph.D. Dissertation*, University of Illinois at Urbana-Champaign, Illinois.

[11] Miller DJ, Fahnestock LA and Eatherton MR (2011): Self-centering buckling-restrained braces for advanced seismic performance. *Structures Congress*, Nevada, US.

[12] Miller DJ, Fahnestock LA and Eatherton MR (2012): Development and experimental validation of a nickel-titanium shape memory alloy self-centering buckling-restrained brace. *Engineering Structures*, 40(2012): 288-298.

[13] Christopoulos C, Tremblay R, Kim HJ and Lacerte M (2008): Self-centering energy dissipative bracing system for the seismic resistance of structures: development and validation. *Journal of Structural Engineering*, 134(1): 96-107.

[14] Zhu SY and Zhang YF (2008): Seismic analysis of concentrically braced frame systems with self-centering friction damping braces. *Journal of Structural Engineering*, 134(1): 121-131.

[15] Tremblay R, Lacerte M and Christopoulos C (2008): Seismic response of multistory buildings with self-centering energy dissipative steel braces. *Journal of Structural Engineering*, 134(1): 108-120.

[16] Erochko J and Christopoulos C (2014): Seismic response of six-story steel frame building with self-centering energy-dissipative (SCED) braces combined with linear viscous dampers. *Tenth U.S. National Conference on Earthquake Engineering, Frontier of Earthquake Engineering*, Anchorage, Alaska.